International Journal of Sciences: Basic and Applied Research (IJSBAR)

ISSN 2307-4531
(Print & Online)

http://gssrr.org/index.php?journal=JournalOfBasicAndApplied

Effect of Inlet Width on Turbulent Flow in a Vented Cavity with an Isothermal Vertical Wall

Bouaraour Kamel[a]*, Belaid Abdelfateh[b]

[a]*Department of Sciences and Technology, Ghardaia University. Ghardaia. Algeria*

[b]*Laboratory of Transport Engineering and Environment, Constantine University 1. Constantine. Algeria*

[a]*Email: bouaraourk@yahoo.fr*

[b]*Email: snseh15@gmail.com*

Abstract

A two-dimensional, turbulent mixed convection flow in vented square cavity is investigated numerically using a computational fluid dynamics (CFD) Fluent code. The vented cavity walls were considered adiabatic, except the vertical wall on left, which was kept at high temperature than the ambient temperature. A low Reynolds number RNG based k-ε turbulence model is used to solve the governing equations. Results are reported for a fixed Reynolds number (Re = 10^4) and for different Grashof numbers varied from 10^8 to 5.10^9. Different values of inlet width are tested: h=0.02, h=0.05, h=0.08 and h=0.1 m. Such convection inside a cavity is characterized by the formation of boundary layers along the heated wall with an encircled recirculating core region. The computed flow patterns, thermal field, variation of the local Nusselt number and the average Nusselt number are reported. It was concluded that flow behavior are changed by varying the inlet width for the same Grashof number.

Keywords: Mixed turbulent convection; vented cavity; k-ε model

---

* Corresponding author. Tel: +213 552977385, Fax: +213 29258149

E-mail address: bouaraourk@yahoo.fr

1. Introduction

Fluid flow and heat transfer in ventilated cavities can be found in many engineering applications such as cooling electronic devices, fire propagation in rooms and thermal comfort inside buildings under natural or forced ventilation conditions. The performance of numerical methods is highly required for describing turbulent fluid flow and heat transfer inside cavities. Concerning the use of turbulence models, many studies use the low Reynolds number (LRN) models instead of the standard k-ε model described by Launder and Spalding [1].

According to the literature review, many numerical studies have analyzed a number of governing parameters in vented cavities and rooms such as room aspect ratio effects [2-3], inlet velocity and enclosure width [4] and inlet turbulent intensity [5]. LRN k-ε models were tested for wide range of Reynolds numbers, where higher capability for predicting turbulent quantities and heat transfer is shown. However; LRN models have their limitations, especially when a fine grid resolution is needed to solve the viscous sub-layer, which need a significant computing time and memory storage. For these raisons, performance of computational fluid dynamics (CFD) codes is needed.

Velocity characteristics throughout a long slot ventilated enclosure is investigated experimentally and numerically [6], where the inlet and outlet sections are located on the same side. Computations were carried out using Fluent code for two configurations with the same aspect ratio, but with different positions and sizes of the inlet. The authors conclude that the use of the second moment closure predict airflow patterns and flow separation better than the two- equation models. Using the same CFD code, a numerical study was carried out by Saeidi and Khodadadi [7] concerning the forced convection in a vented square cavity in the laminar regime. In order to understand the complicated flow and thermal fields in such a configuration, 108 cases have been studied by fixing the inlet and varying the outlet location and Reynolds number. Numerical results give the most effective location for the outlet port that accommodates maximum heat transfer and minimum pressure drop. A great attention has been focused on mixed convection from a heater in a ventilated cavity due to its engineering applications. A combined experimental and numerical study is reported by T.V. Radhakrishnan et al [8]. Many locations and sizes of the heater are tested to improve the heat transfer performance in a rectangular cavity that has an air inlet and an outlet port. The aim of this study was to find the optimum location of the heater in order to have the maximum cooling. Numerical results showed good agreement with experimental data. To determine the good ventilation configuration and to analyze temperature distribution inside a rectangular cavity, mixed turbulent study is reported by J. Xaman et al [9]. The right vertical wall of the cavity is exposed to a constant heat flux, and the other walls are insulated. Four locations of air exhaust are tested with a varying Reynolds number from 2.10^3 to 4.10^4. The authors made a correlation relation between Nusselt number and Reynolds number for each configuration, and found the appropriate thickness of the active wall to minimize thermal load gains inside the room and to reduce the efforts made on ventilation to remove heat, which have a great practical interest.

In this paper, a two-dimensional study based on Fluent code is carried out to simulate the turbulent ventilation and heat transfer inside a square cavity with inlet and outlet vents located on opposite sides. The turbulent air flow and mixed convection heat transfer inside the vented cavity is modeled in terms of the RNG k-ε model.

The effects of varying the vent size and Grashof number related to the heated wall are reported. The same configuration is studied numerically by D. Angirasa but in the laminar case [10].

2. Configuration

The mixed turbulent flow will be carried out in a square vented cavity with a height H of1 m. The left vertical wall is kept at higher temperature T_w than the ambient temperature T_0, whereas the other walls are thermally insulated. Air enters to the cavity at 288.16 K through as mall vent located at the bottom of the lower wall. Inlet vent has a variable width h and outlet vent have a fixed width equal to 0.1 m. Figure 1 shows the configuration of the considered cavity.

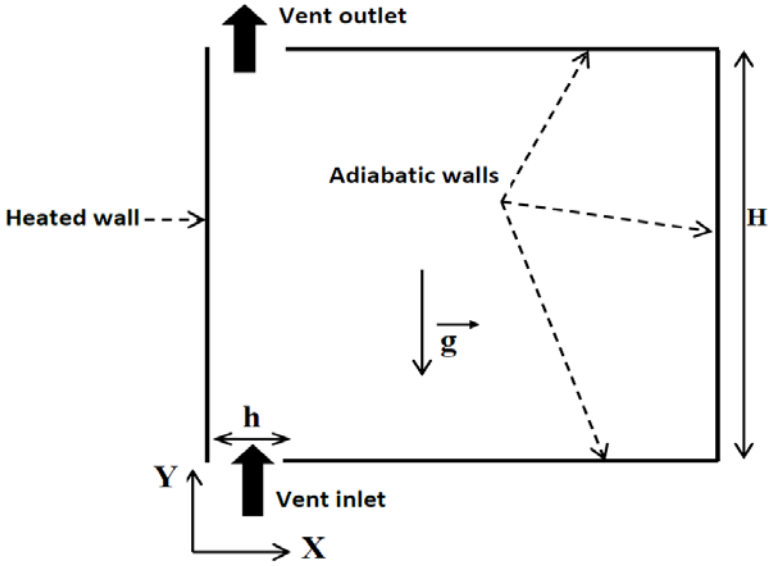

Figure 1: Configuration and coordinate system

3. Governing equations and boundary conditions

The governing equations for turbulent mixed convection flows is described mathematically by the Reynolds averaged Navier-Stokes equations (RANS), and by energy equation. The Boussinesq approximation which assumes constant proprieties for the fluid except the density in the buoyancy term of governing equations is considered. The RANS equations for the velocity and temperature field are as follows:

$$\frac{\partial(\rho U_i)}{\partial X_i} = 0 \qquad (1)$$

$$\frac{\partial(\rho U_i)}{\partial t} + \frac{\partial(\rho U_i U_j)}{\partial X_j} = -\frac{\partial P}{\partial X_i} + \frac{\partial}{\partial X_j}\left[\mu \frac{\partial U_i}{\partial X_j} - \rho \overline{u_i u_j}\right] + g_i(\rho - \rho_\infty) \qquad (2)$$

$$\frac{\partial(\rho c_p T)}{\partial t} + \frac{\partial(\rho c_p T U_j)}{\partial X_j} = \frac{\partial}{\partial X_j}(\lambda \frac{\partial T}{\partial X_j} - \rho c_p \overline{T' u_j}) \qquad (3)$$

Where turbulence stress and turbulent heat flux are approximated respectively as:

$$-\rho\overline{u_i u_j} = \mu_t\left(\frac{\partial U_i}{\partial X_j} + \frac{\partial U_j}{\partial X_i}\right) - \frac{2}{3}\rho\delta_{ij}K \qquad (4)$$

$$-\rho c_p\overline{T'u_j} = c_p\frac{\mu_t}{\mathrm{Pr}_t}\frac{\partial T}{\partial X_j} \qquad (5)$$

Where the Kronecker delta is given by $\delta_{ij}=1$ if (i=j) and $\delta_{ij}=0$ if ($i \neq j$). Turbulence is modeled with the RNG based k- ε model derived from the instantaneous Navier-Stokesequations, using a mathematical technique called renormalization group RNG methods. The RNG model is an eddy-viscosity model similar to the standard k-ε model, but incorporates near wall turbulence anisotropy and non-local pressure-strain effects. It is a general low-Reynolds number turbulence model that is valid all the way up to solid walls, and therefore does not need to make use of wall functions.

$$\frac{\partial(\rho K)}{\partial t} + \frac{\partial(\rho U_i K)}{\partial X_i} = \frac{\partial}{\partial X_i}\left(\mu + \frac{\mu_t}{\sigma_K}\frac{\partial K}{\partial X_i}\right) + P_K + G_K - \rho\varepsilon \qquad (6)$$

$$\frac{\partial(\rho\varepsilon)}{\partial t} + \frac{\partial(\rho U_i \varepsilon)}{\partial X_i} = \frac{\partial}{\partial X_i}\left(\mu + \frac{\mu_t}{\sigma_\varepsilon}\frac{\partial \varepsilon}{\partial X_i}\right) + C_{\varepsilon 1}\frac{\varepsilon}{K}\left(P_K + C_{\varepsilon 3}G_K\right) - C_{\varepsilon 2}\frac{\rho\varepsilon^2}{K} - R_\varepsilon \qquad (7)$$

The analytical derivation results in a model with constants that are different from those employed in the standard k- ε model, where P_k and G_k are the sheer production of turbulence kinetic energy and the buoyant production/destruction of turbulence kinetic energy respectively. R_ε is an additional term related to mean strain and turbulence quantities as:

With:

$$R_\varepsilon = \frac{C_\mu\rho\eta^3\left(1-\frac{\eta}{\eta_0}\right)}{1+\beta'\eta^3}\frac{\varepsilon^2}{K} \qquad (8)$$

$$\eta = \sqrt{2S_{ij}S_{ij}}\,\frac{K}{\varepsilon} \qquad (9)$$

And the strain tensor is defined as:

$$S_{ij} = \frac{1}{2}\left(\frac{\partial U_i}{\partial X_j} + \frac{\partial U_j}{\partial X_i}\right) \qquad (10)$$

The constants of this model are presented in table 1.

The boundary conditions for the considered problem can be expressed as:

- The velocity at the gap of the inlet is: $V=V_{in}$ and $U_{in}=0$. Turbulent kinetic energy and dissipation at the inlet

are respectively: $K_{in}=1.5(V_{in}I_0)^2$ and $\varepsilon_{in}=K_{in}^{1.5}/\ell$. ℓ: is a turbulent length scale (ℓ=h/10 m) andI_0 is the inlet turbulent intensity (I_0=10%).

- At the gap of the outlet, gradients of all variables in the y- direction are set to zero.
- The velocity boundary conditions are fixed as zero over the solid walls.
- Thermal boundary conditions are: $\partial T/\partial n= 0$ for the adiabatic walls, where n denote the coordinate normal to the boundary.
- Temperature of the heated wall is $T=T_w$ and the inlet air temperature is $T=T_0$.

Table 1: Constants of RNG k-ε model

C_μ	$C_{\varepsilon 1}$	$C_{\varepsilon 2}$	η_0	β'
0.0845	1.42	1.68	4.38	0.012

4. Numerical methods

The governing equations are discretized using finite volumes schemes and the solver is the commercial CFD code FLUENT 6.3. The velocity components are calculated at a staggered grid while the scalar variables are calculated at the main grid (not staggered). For coupling of mass and momentum equations, SIMPLE algorithm with second order up winding for momentum and energy solution was considered [11]. The discretization of pressure is based on the PRESTO! scheme. The convergence criterion was taken 5.10^{-6} for the residual of each equation. We have used relaxation factors of 0.7 for velocities, 0.8 for temperature and turbulent values and 0.3for the pressure. The current numerical CFD code has been applied with success to validate many numerical studies in the forced turbulent cases [7], natural turbulent cases [12-13] and mixed turbulent cases [8]-[14].

5. Results and discussion

To understand flow field and heat transfer features inside the cavity, four Grashof numbers are considered: Gr = 10^8 , 5.10^8 , 10^9 and 5.10^9 . The effect of varying inlet width is also studied for a fixed position of the inlet and the outlet vent. Reynolds number based on the inlet width and the inlet velocity is fixed at 10^4 and Prandtl number is 0.71.

5.1. Grid independence and code validation

Numerical results are obtained with non-uniform meshes of different grid sizes: 130 × 80,150 × 100 and 164 × 125. The wall y^+ values are less than 1, so the viscous sub layer is resolved adequately. For Gr = 5.10^8 , the maximum deviation was less than 1% for the maximum velocity and less than 2% for the average Nusselt number between the two last meshes. To validate the mathematical model and numerical methods, it has been tested with the experimental results of the natural turbulent convection in a square cavity available in the literature [15], where vertical walls are maintained at uniform and different temperatures, while the horizontal walls are kept insulated. The cavity has a height of 0.75 m and a width of 0.75 m and the temperature difference

was 40 K, which gives a Rayleigh number of: $1.58x10^9$. The number of iterations needed to converge was more than 10^6. The resulting streamlines and isotherms are shown in figure 2 and figure 3 respectively.

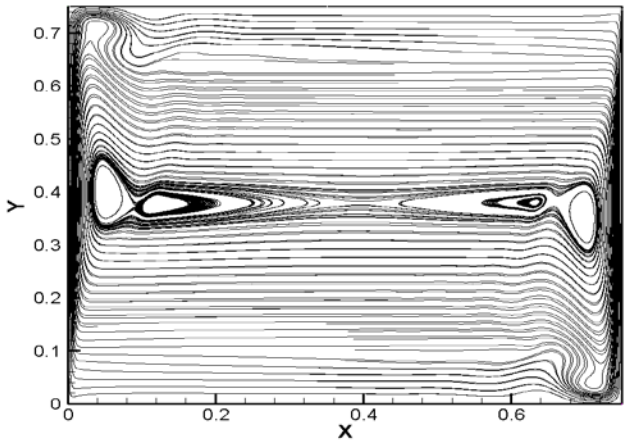

Figure 2: Streamlines for $Ra=1.58x10^9$.

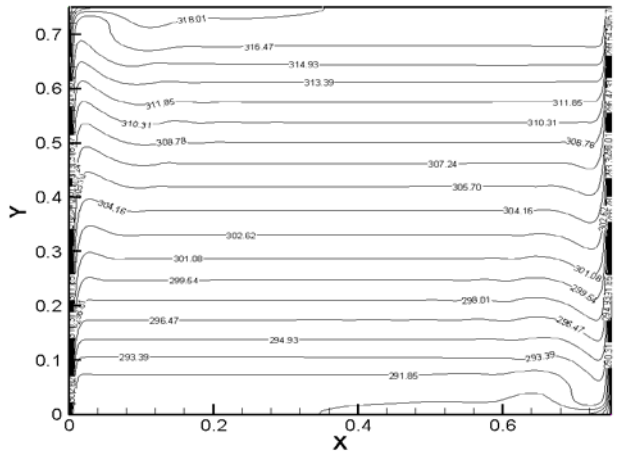

Figure 3: Isotherms for $Ra=1.58x10^9$.

A non-uniform mesh of 150 × 120 grid points is used to simulate natural turbulent convection inside the cavity. Good agreement was found between the numerical results of temperature profile at mid-height of the cavity and the experimental results of Tian et al [15] as shown in figure 4.

5.2. Flow field in the cavity

Interaction between airflow and pressure gradient imply the presence of primary and secondary recirculation.

The compute streamlines patterns inside the cavity are shown in figure 5.

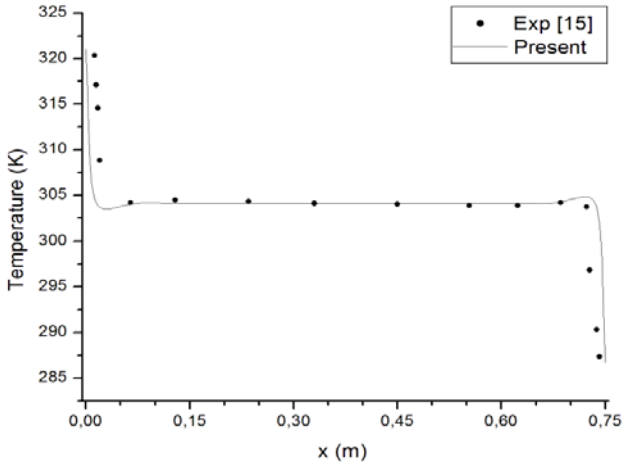

Figure 4: Comparison of predicted temperature profile at mid-height of the square cavity with experimental data [15].

For a Grashof number of 5.10^9 , a main vortex with clockwise recirculation that occupies more than 90% of the cavity can be seen for the four inlet widths. Three small vortices with counterclockwise recirculation can be observed in the cavity for h=0.02 m. Two vortices are located at the corners of the right wall and a third one is located just right the incoming flow at the entrance. For h=0.05 m, in addition to the main vortex, two small secondary vortices located at the upper right corner and the lower right corner can be observed. Similar streamlines can be observed for h=0.08 m and h=0.1 m, with increasing in size of the two small counterclockwise vortices. The center of the main vortex moved right when varying inlet width from h=0.02 m to h=0.1 m.

Varying Grashof number from 10^8 to 5.10^9 does not give significant influence on the vertical velocity profiles. The same behavior have been seen especially close to the vertical wall, where there is a thin boundary layer that grows in thickness as the flow travels up as indicated in figure 6.

For the same inlet width, the highest velocity values are always close to the vertical wall. The dominant flow is along the heated wall, and recirculating flow in the core is weaker. Far from the heated wall, vertical velocity profiles at mid-height of the cavity become more and more uniform especially for the largest inlet widths (h=0.08 m, h=0.1 m) as shown in figure 7.

For the same inlet width, the flow field appeared very similar for the various Grashof numbers studied. This means that fluid flow is dominated by fluid velocity rather than buoyancy effects induced by the temperature gradient. An example of streamlines for h=0.02 m is shown in figure 8.

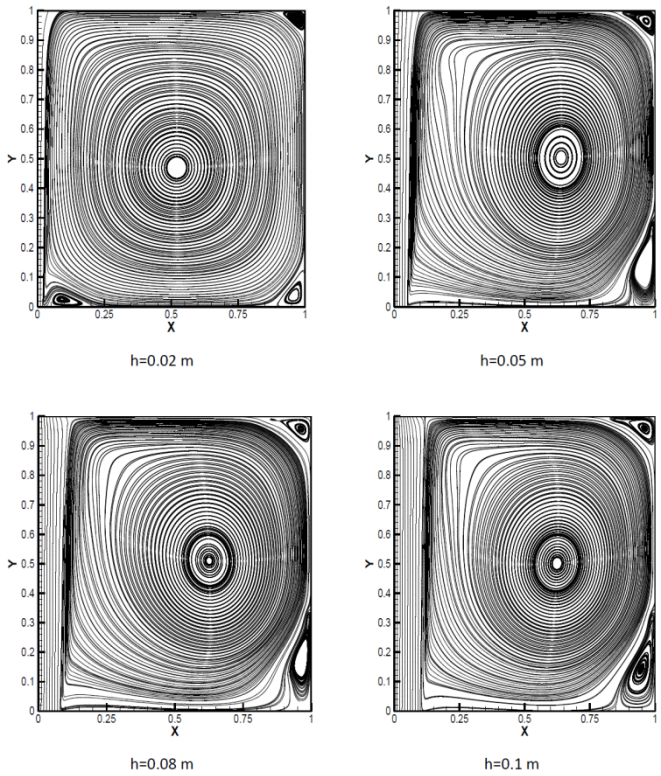

Figure 5: Streamlines for Gr=5.10^9.

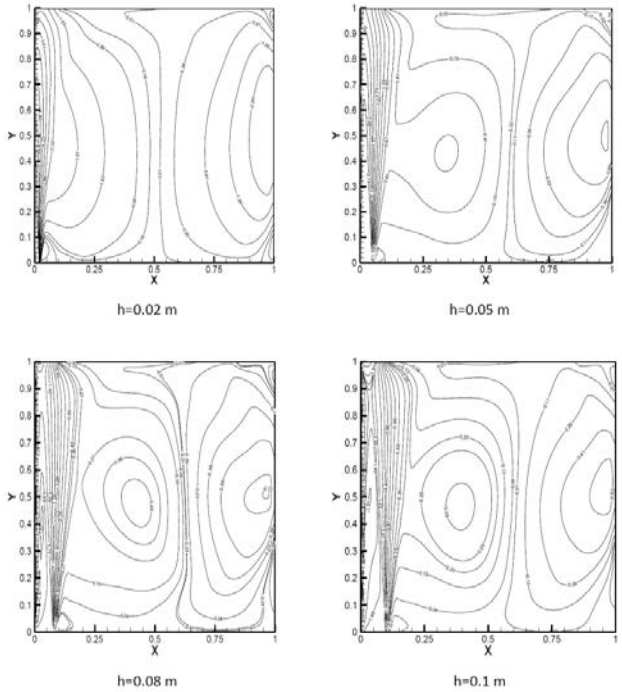

Figure 6: Vertical velocity contours for Gr=5.10^9.

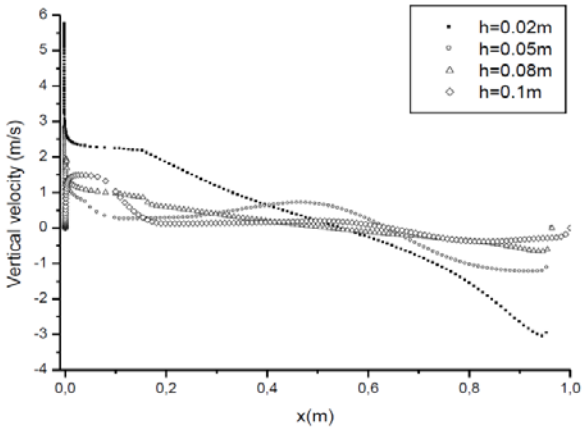

Figure 7: Vertical velocity at mid-height for Gr=5.10^9.

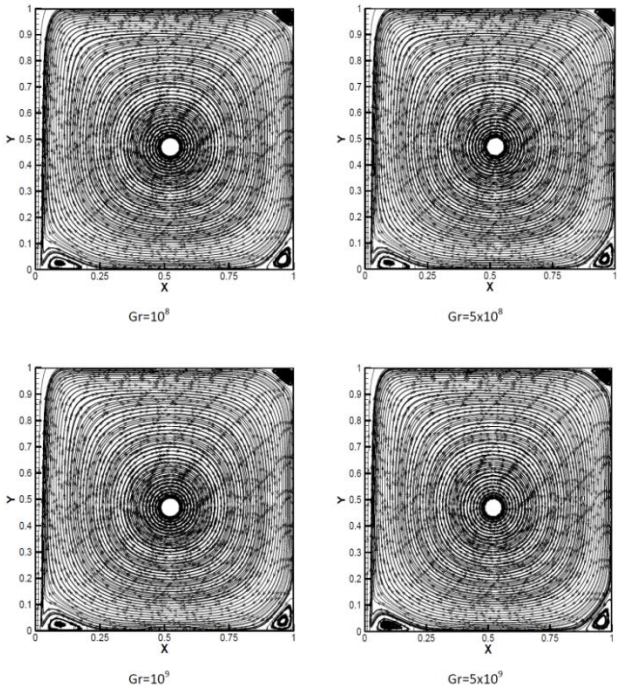

Figure 8: Streamlines for h=0.02 m.

5.3. Temperature field in the cavity

Isotherms for the four considered inlet widths at Gr = 5.10^9 are shown in figure 9. For h=0.02m, the isothermals show a tendency to form circles that run from the inlet and returning to the inlet over the heated vertical wall first and then over the three adiabatic walls. A stratification zone that occupied from 15% to 20% of the cavity is clearly appeared in the upper part of the cavity. By increasing inlet width, the isothermals are pushed towards

the right side of the cavity.

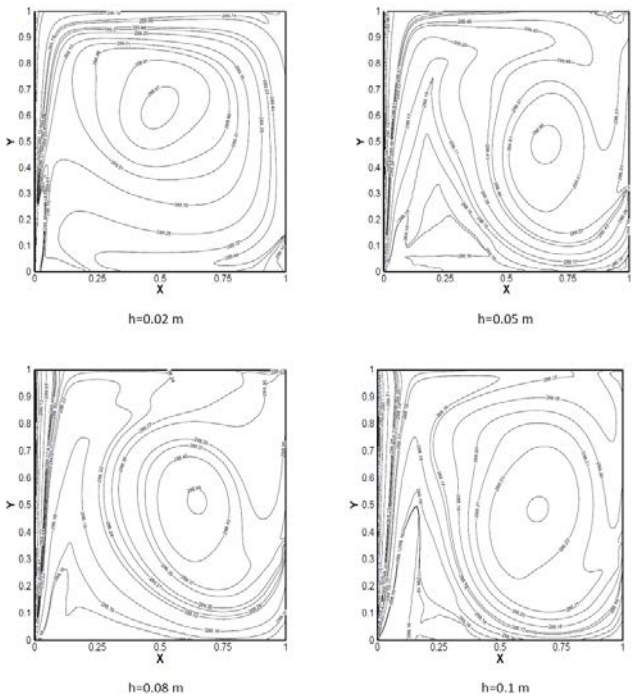

Figure 9: Isotherms for Gr = 5.10^9.

5.4. Local Nusselt number on the heated wall

Local Nusselt number which evaluates heat transfer of the heated wall is defined as:

$$Nu = -\frac{H}{T_w - T_0}\frac{\partial T}{\partial x}\bigg|_{x=0} \qquad (11)$$

Local Nusselt number variation at Gr = 5.10^9 is presented in figure 10. It is evident that Nusselt number is larger near the heated wall where temperature gradient is important. Nu number decreases monotonically with distance y along the wall. The highest Nusselt numbers are located in the lowest end of the heated wall for all inlet widths considered.

The average Nusselt number of the heated vertical wall is defined as:

$$\overline{Nu} = \frac{1}{H}\int_0^H Nu.dy \qquad (12)$$

Variation of the average Nusselt number for Gr = 5.10^9 is presented in figure 11. It is observed that average Nusselt decreases almost linearly with inlet width, especially between h=0.05 m and h=0.1 m.

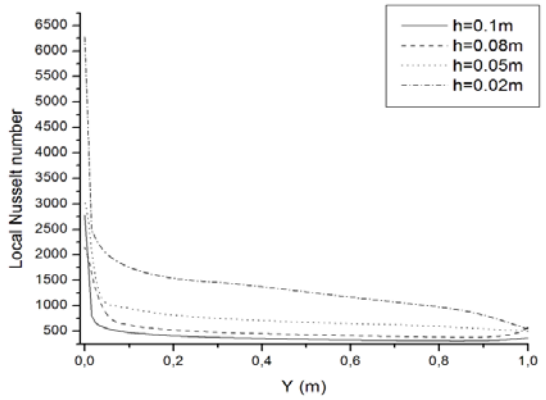

Figure 10: Local Nusselt number distribution for Gr = 5.10^9.

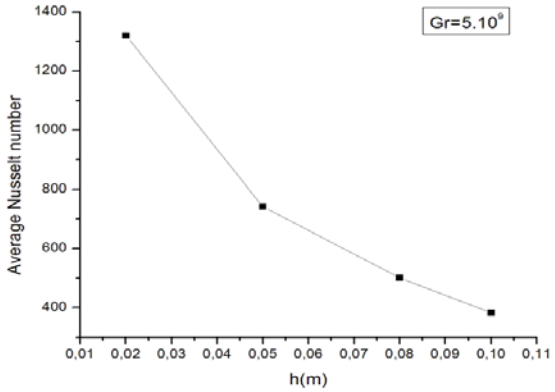

Figure 11: Average Nusselt for Gr = 5.10^9

6. Conclusion

In this paper a numerical study of mixed turbulent convection inside a vented cavity was presented. Reynolds number based on the inlet width and the inlet air velocity is fixed at 10^4.Results are discussed for different Grashof numbers varied from 10^8 to 5.10^9 and four values of inlet width are tested : h=0.02 m, h=0.05 m, h=0.08 m and h=0.1 m. It was found that the variation of the inlet width affects the airflow patterns, velocity characteristics and heat transfer inside the vented cavity. The following remarks can be made:

- For the same Grashof number, maximum velocities are always found for the smallest inlet width.
- The considered Reynolds number and Grashof numbers make the flow inside the cavity dominated by inertia forces rather than by buoyancy forces induced by temperature gradient.
- Vertical velocity profiles have the same behavior near the heated wall for the same inlet width, and for many vertical positions. Far from the heated wall, small difference is observed.

- The average Nusselt number for the heated wall decreases almost linearly with the inlet width.

References

[1] B.E. Launder and D.B. Spalding, The numerical computation of turbulent flow, Computer Methods in Applied Mechanics and Energy 3, 269-289, 1974.

[2] J. J. Costa, L.A. Oliveira and D. Blay, Test of several versions for the k-ε type turbulence modeling of internal mixed convection flows, International Journal of Heat and Mass Transfer42, 4391-4409, 1999.

[3] J. J. Costa, L. A. Oliveira and D. Blay, Turbulent airflow in a room with a two-jet heating-ventilation system: a numerical parametric study, Energy and Buildings 32, 327-343, 2000.

[4] A. Behzadmehr, N. Galanis and C.T. Nguyen, Predicted effects of inlet turbulent intensity on mixed convection in vertical tubes with uniform wall heat flux, International Journal of Thermal Sciences 45, 433-442, 2006.

[5] Fu-Yun Zhao, Di Liu and Guang-Fa Tang, Multiple steady fluid flows in a slot-ventilated enclosure, International Journal of Heat and Fluid Flow 29, 1295-1308, 2008.

[6] J. Moureh and D. Flick, Airflow characteristics within a slot-ventilated enclosure, International Journal of Heat and Fluid Flow 26, 12-24, 2005.

[7] S. M. Saeidi and J. M. Khodadadi, Forced convection in a square cavity with inlet and outletports, International Journal of Heat and Mass Transfer 49, 1896-1906, 2006.

[8] T. V. Radhakrishnan, A. K. Verma, C. Balaji and S. P. Venkateshan, An experimental andnumerical investigation of mixed convection from a heat generating element in a ventilatedcavity, Experimental Thermal and Fluid Science 32, 502-520, 2007.

[9] J. Xaman, J. Tunb, G. AÂlvareza, Y. Chaveza and F. Noha, Optimum ventilation based onthe overall ventilation effectiveness for temperature distribution in ventilated cavities, International Journal of Thermal Sciences 48, 1574-1585, 2009.

[10] D. Angirasa, Mixed convection in a vented enclosure with an isothermal vertical surface,Fluid Dynamics Research 26, 219-233, 2000.

[11] S. V. Patankar, Numerical heat transfer and fluid flow, Mac Graw Hill, New York, 1980.

[12] R. Harish and K. Venkatasubbaiah, Numerical simulation of turbulent plume spread inceiling vented enclosure, European Journal of Mechanics B/Fluids 42, 142-158, 2013.

[13] S. Wanga, Z. Shena and L. Gub, Numerical simulation of buoyancy-driven turbulent ventilation in attic

space under winter conditions, Energy and Buildings 47, 360-368, 2012.

[14] J. Moureh, M. Tapsoba and D. Flick, Airflow in a slot-ventilated enclosure partially filled with porous boxes: Part II- Measurements and simulations within porous boxes, computers and fluids 38, 206-220, 2009.

[15] Y. S. Tian and T. G. Karayiannis, Low turbulence natural convection in an air filled squarecavity: Part I: The thermal and fluid flow fields, International Journal of Heat and Mass Transfer 43, 849-866, 2000.